acta physica slovaca vol. 53 No. 2, 95 – 104 April 2003

OPTICAL CONSTANTS OF ZnTe AND ZnSe EPITAXIAL THIN FILMS [*]

D. Franta[*,1], I. Ohlídal[†], P. Klapetek[†,‡], A. Montaigne-Ramil[§],
A. Bonanni[§], D. Stifter[§], H. Sitter[§]
[*] *Laboratory of Plasma Physics and Plasma Sources, Faculty of Science, Masaryk University, Kotlářská 2, 611 37 Brno, Czech Republic*
[†] *Department of Physical Electronics, Faculty of Science, Masaryk University, Kotlářská 2, 611 37 Brno, Czech Republic*
[‡] *Czech Metrology Institute, Okružní 31, 638 00 Brno, Czech Republic*
[§] *Institute of Semiconductor Physics, Johannes Kepler University, Altenbergerstrasse 69, A-4040 Linz, Austria*

Received 4 December 2002, accepted 22 January 2003

In this paper the spectral dependences of the optical constants, i. e. refractive index and extinction coefficient, are presented within the spectral region 220–850 nm. For determining these spectral dependences a multi-sample modification of the combined optical method based on a simultaneous interpretation of experimental data corresponding to variable angle spectroscopic ellipsometry and near-normal spectroscopic reflectometry is used. Further, physical models and an iterative procedure enabling us to determine the spectral dependences of the optical constants of both the epitaxial films are described in detail. The spectral dependences of the optical constants are introduced in the forms of curves and tables.

PACS: 78.20.Ci, 78.66.Hf

1 Introduction

Single crystal films of ZnSe and ZnTe are frequently employed in various branches of applied research and industry. For example, they are used to create optical waveguides on the basis of a three-layer ZnSe/ZnTe/ZnSe system prepared on single-crystal GaAs substrate. These films are also employed in many applications in optoelectronic and integrated optics. Both the ZnTe and ZnSe epitaxial films utilized for these purposes must exhibit high optical quality. Therefore efficient optical methods must be used to check this quality. Methods of spectroscopic ellipsometry belong to a number of methods that enables us to carry out reliable precise optical analysis of ZnSe and ZnTe thin films [1–7]. It is known that a multi-sample modification of variable angle spectroscopic ellipsometry (VASE) intensifies the efficiency of VASE applied for a single sample [6–11]. Moreover, it is known that the efficiency of the multi-sample modification of VASE is further intensified when a spectral dependence of the reflectance measured at near-normal incidence is added to the ellipsometric data corresponding to VASE. Thus, the most efficient method

---

[*] Presented at Workshop on Solid State Surfaces and Interfaces III, Smolenice, Slovakia, November 19 – 21, 2002.

[1] E-mail address: franta@physics.muni.cz

is the multi-sample modification used for the combined method based on a simultaneous treatment of both VASE and NNSR data (NNSR denotes near-normal spectroscopic reflectometry). Therefore we used the multi-sample modification of VASE or multi-sample modification of the combined method (VASE plus NNSR) to carry out complete optical characterization of several samples of the ZnTe/GaAs and ZnSe/GaAs systems that differed in the values of the thicknesses of the ZnSe and ZnTe films. In this optical characterization relatively complicated physical models of ZnSe and ZnTe films were employed. These models contain rough overlayers that lay on the upper boundaries of ZnSe and ZnTe films. Moreover, in the case of the ZnTe films the profiles of their optical constants across these films were assumed. Using a relatively complicated iterative procedure the spectral dependences of the refractive index and extinction coefficient of both the films were determined within the spectral region formed by the near-UV and visible regions (220–850 nm).

2 Experiment

2.1 Preparation of the samples

The films of ZnSe were prepared by molecular beam epitaxy (MBE) on (100) GaAs single crystal substrates. The temperature of the substrates was in the range 300 to 350°C. The flux of Zn and Se atoms was monitored with a reference gauge, placed close to the sample holder. The beam equivalent pressure for Zn and Se was $1\text{–}2 \times 10^{-7}$ Torr and $4\text{–}16 \times 10^{-7}$ Torr, respectively. The Se:Zn-ratio was within the interval 5–14. The growth rate was between 2.6–8.4 nm/min. A (2×1) reconstructed surface structure appears on the Se-covered surface which was observed by reflection high-energy electron diffraction. Six samples of ZnSe films different in thickness were analyzed.

The epitaxial films of ZnTe were prepared by MBE on (100) GaAs single crystal substrates. The temperature of the substrates was of 300°C. The flux of Zn and Te atoms was monitored in the same way as in the case of ZnSe films. The beam equivalent pressure for Zn and Te was $1\text{–}2 \times 10^{-7}$ Torr and $4\text{–}16 \times 10^{-7}$ Torr, respectively. The growth rate was between 4–8 nm/min. Five samples of ZnTe films different in thickness were optically investigated.

2.2 Experimental arrangements

The spectral dependences of the ellipsometric quantities were measured using a Jobin–Yvon UVISEL DH10 phase-modulated ellipsometer within the spectral region 220–850 nm. For this spectral region the ellipsometric spectral dependences were measured for five angles of incidence laying within the interval 55–75° (i. e. for the angles of 55°, 60°, 65°, 70°, 75°). The spectral dependences of the reflectance were measured using a spectrophotometer Perkin–Elmer Lambda 45 within the same spectral region as the ellipsometric quantities. The reflectance measurements were realized for the angle of incidence of 6°.

3 Models of the ZnSe and ZnTe films

3.1 ZnSe films

The physical model of the ZnSe films employed in this paper is specified by the following assumptions:

- Both the film and substrate are formed by homogeneous and isotropic materials from the optical point of view.
- The ambient is formed by a non-absorbing homogeneous isotropic material (e. g. by air).
- The upper boundary of the film is randomly rough and, moreover, it is covered with a very thin overlayer (i. e. it is assumed that the overlayer is formed by an identical thin film whose both the boundaries are identically rough [12]).
- The roughness of the upper boundary is generated by the stationary isotropic stochastic process.
- The values of the heights of the irregularities of the upper boundary of the film are considerably smaller than the wavelength λ of incident light.
- The boundary between the GaAs substrate and ZnSe film is smooth.

3.2 ZnTe films

The model of the ZnTe films is formed by the GaAs substrate covered with the double layer consisting of an absorbing inhomogeneous thin film representing the ZnTe film and the native oxide layer (NOL). The inhomogeneity of the film corresponds to a profile of the complex refractive index across the film. The inhomogeneous film and the NOL are assumed to be isotropic. Both the boundaries of the NOL were assumed to be rough (the NOL was approximated by the identical thin film as well). The boundary between the GaAs substrate and inhomogeneous film is supposed to be smooth. Within this model the profile expressed by the following equation is assumed:

$$\hat{n}(z) = \sqrt{\hat{n}_{\mathrm{a}}^2\,[1 - p(z)] + \hat{n}_{\mathrm{b}}^2\,p(z)} \qquad \text{for} \quad z < b \tag{1}$$

and

$$\hat{n}(z) = \sqrt{\hat{n}_{\mathrm{f}}^2\,[1 - p(z)] + \hat{n}_{\mathrm{b}}^2\,p(z)} \qquad \text{for} \quad z \geq b \tag{2}$$

where function $p(z)$ is defined as

$$p(z) = \frac{z}{b}\mathrm{e}^{1 - z/b}, \tag{3}$$

where b is a parameter, $\hat{n}_{\mathrm{a}}$ denotes the refractive index of the film at the boundary between the substrate and this film, $\hat{n}_{\mathrm{b}}$ denotes the refractive index of the film in the distance b above the substrate and $\hat{n}_{\mathrm{f}}$ represents the refractive index of the film in relatively large distance above the substrate. The complex refractive indices are expressed as follows: $\hat{n}(z) = n(z) - \mathrm{i}k(z)$, $\hat{n}(0) = \hat{n}_{\mathrm{a}} = n_{\mathrm{a}} - \mathrm{i}k_{\mathrm{a}}$, $\hat{n}(b) = \hat{n}_{\mathrm{b}} = n_{\mathrm{b}} - \mathrm{i}k_{\mathrm{b}}$, $\hat{n}(z) = \hat{n}_{\mathrm{f}} = n_{\mathrm{f}} - \mathrm{i}k_{\mathrm{f}}$ for a sufficiently large value of z (strictly for $z \to \infty$). The symbol z denotes the variable corresponding to the axis perpendicular to the boundaries and n and/or k denotes the corresponding real refractive index and/or corresponding extinction coefficient. The foregoing model of the profile of the ZnTe film was selected from several profile models examined on the basis of the best agreement between both the theoretical and experimental data. In this model is again supposed that the ambient is formed by air.

4 Data processing

At the data processing concerning both the ZnSe and ZnTe epitaxial films we used the least squares method (LSM) within the iterative procedure mentioned above. Each of the iterations contained two steps. In the first step the values of the optical constants of ZnSe and ZnTe films were determined by the LSM using the values of the optical quantities measured for individual wavelength in the spectral region of interest. Thus, the values of the optical constants of both the films were determined separately for each wavelength using experimental data that correspond to all the samples and to all the incidence angles. The thicknesses of the ZnSe and ZnTe films and the parameters describing the overlayers were fixed at the values estimated (the values of the roughness parameters were estimated by AFM, the thickness values of the ZnSe and ZnTe films were estimated from technological conditions of MBE used and thickness values of the overlayers were assumed to be 2 nm). The values of the optical constants of the overlayers of ZnSe and/or ZnTe films were searched on basis of the several formulae and/or were fixed in the values of the optical constants corresponding to amorphous $(Ga,As)_2O_3$ (for details see Refs. [6, 7, 13]). In the second step the optical constants of the films were fixed at the values obtained from the first step. The values of the thicknesses of the ZnSe and ZnTe films and the other parameters corresponding to the overlayers of all the samples were found by the LSM that was applied to all the ellipsometric and reflectometric data measured. Note that the thicknesses of the overlayers on the upper boundaries of all the ZnTe films were identical. The same assumption was taken into account for the ZnSe films as well.

In the following iterations the ZnSe and ZnTe film thicknesses and the other parameters corresponding to overlayers fixed in the first step were taken from the previous iteration and the values of the optical constants of ZnSe and ZnTe films were found in the way described above (see the first step). The second step of the following iterations was identical to the second one in the first iteration.

The theoretical values of the ellipsometric quantities and reflectance were calculated using matrix formalism [14, 15]. In this matrix formalism the overlayers lying on the rough upper boundaries of the ZnSe and ZnTe films were respected by means of Rayleigh–Rice theory [16, 17]. For calculation of the optical quantities characterizing inhomogeneous thin film was used a new mathematical procedure based on the matrix formalism and Drude approximation (for details see Ref. [18]).

In the data treatment the values of the optical constants of the GaAs substrates were fixed at values from the literature [19].

5 Results and discussion

Using the numerical procedure explained in the foregoing section the optical constants, i. e. the refractive index n and extinction coefficient k, of the ZnTe films were determined within the spectral region 230–850 nm. These spectral dependences of n and k are plotted in Fig. 1. In detail the values of n and k for the selected wavelengths of the spectral region are summarized in Tab. 1.

The spectral dependences of the optical constants of the ZnSe films obtained in the spectral region 220–850 nm are plotted in Fig. 1. The values of n and k corresponding to these spectral dependences are summarized in Tab. 2.

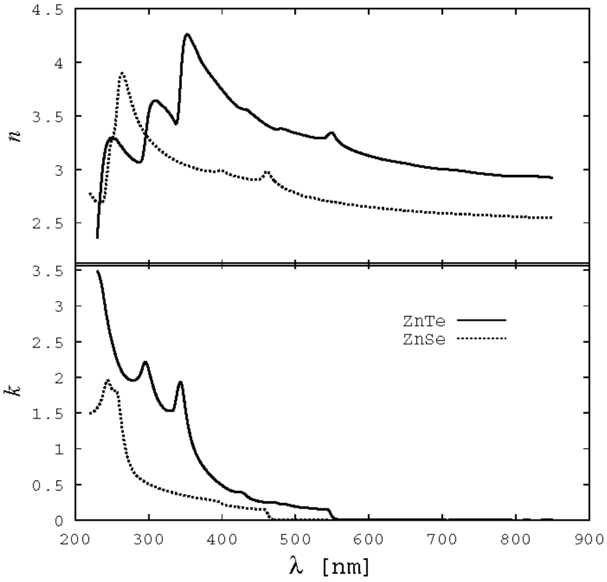

Fig. 1. The spectral dependences of the refractive index n and extinction coefficient k of the ZnTe and ZnSe films.

As for the ZnTe films the spectral dependences of n_{f} and k_{f} are taken as the true spectral dependences of the optical constants of these films (see Eqs. (1)–(3)), i. e. $n_{\mathrm{f}} = n$ and $k_{\mathrm{f}} = k$. In a forthcoming paper it will be shown that these optical constants, i. e. n_{f} and k_{f}, represent the true ones (see Ref. [7]).

6 Conclusion

In this paper the spectral dependences of the optical constants, i. e. the refractive index and extinction coefficient, of the epitaxial thin films of ZnTe and ZnSe prepared by MBE onto single crystal GaAs substrates are presented within the spectral region 230–850 nm and 220–850 nm, respectively. The multi-sample modification of the optical combined method based on the simultaneous interpretation of the experimental data corresponding to VASE and NNSR was used for this purpose. The physical models used to calculate the theoretical values of the ellipsometric quantities and reflectance are described. Moreover, the numerical procedure employed for treating the experimental data is described here as well. The spectral dependences of n and k for both the films are introduced in the forms of the curves and tables.

Acknowledgement: This work was supported within the program AKTION under Contract No. 69p3 and by the Grant Agency of the Czech Republic under contract No. 202/01/1110. The numerical calculations were performed using the SGI Origin3800 High Performance Computer at Johannes Kepler University of Linz.

Tab. 1. The values of the refractive index n and extinction coefficient k of ZnTe layers.

nm	cm^{-1}	eV	n	k
230	43478	5.391	2.355	3.492
232	43103	5.344	2.575	3.447
234	42735	5.299	2.744	3.381
236	42373	5.254	2.912	3.293
238	42017	5.209	3.046	3.174
240	41667	5.166	3.143	3.040
242	41322	5.123	3.209	2.910
244	40984	5.081	3.248	2.794
246	40650	5.040	3.274	2.684
248	40323	4.999	3.292	2.587
250	40000	4.959	3.286	2.504
253	39526	4.901	3.287	2.382
256	39062	4.843	3.276	2.272
259	38610	4.787	3.249	2.187
262	38168	4.732	3.220	2.113
265	37736	4.679	3.194	2.055
268	37313	4.626	3.164	2.017
271	36900	4.575	3.140	1.987
274	36496	4.525	3.119	1.967
277	36101	4.476	3.099	1.961
280	35714	4.428	3.086	1.960
283	35336	4.381	3.073	1.970
286	34965	4.335	3.064	1.999
289	34602	4.290	3.068	2.049
292	34247	4.246	3.117	2.144
295	33898	4.203	3.256	2.212
298	33557	4.161	3.430	2.178
301	33223	4.119	3.554	2.070
304	32895	4.078	3.613	1.952
307	32573	4.039	3.636	1.845
310	32258	4.000	3.641	1.752
315	31746	3.936	3.617	1.644
320	31250	3.875	3.586	1.574
325	30769	3.815	3.551	1.534
330	30303	3.757	3.507	1.527
335	29851	3.701	3.447	1.582
340	29412	3.647	3.496	1.846
345	28986	3.594	3.978	1.909
350	28571	3.542	4.237	1.562
355	28169	3.493	4.244	1.261
360	27778	3.444	4.181	1.056
365	27397	3.397	4.111	0.922
370	27027	3.351	4.029	0.821
375	26667	3.306	3.971	0.742
380	26316	3.263	3.919	0.677
385	25974	3.220	3.874	0.622
390	25641	3.179	3.829	0.569
395	25316	3.139	3.785	0.526
400	25000	3.100	3.742	0.486
405	24691	3.061	3.700	0.452
410	24390	3.024	3.657	0.423
415	24096	2.988	3.622	0.403
420	23810	2.952	3.591	0.394
425	23529	2.917	3.570	0.396
430	23256	2.883	3.560	0.371
435	22989	2.850	3.550	0.329
440	22727	2.818	3.521	0.295
445	22472	2.786	3.493	0.277
450	22222	2.755	3.466	0.264
455	21978	2.725	3.440	0.255
460	21739	2.695	3.416	0.247
465	21505	2.666	3.396	0.246
470	21277	2.638	3.380	0.242
475	21053	2.610	3.373	0.241
480	20833	2.583	3.378	0.224
485	20619	2.556	3.372	0.225
490	20408	2.530	3.361	0.214
495	20202	2.505	3.348	0.202
500	20000	2.480	3.338	0.190
505	19802	2.455	3.329	0.182
510	19608	2.431	3.320	0.179
515	19417	2.407	3.312	0.172
520	19231	2.384	3.302	0.167
525	19048	2.362	3.296	0.162
530	18868	2.339	3.291	0.157
535	18692	2.317	3.290	0.152
540	18519	2.296	3.294	0.149
545	18349	2.275	3.321	0.141
550	18182	2.254	3.342	0.049
555	18018	2.234	3.292	0.014
560	17857	2.214	3.252	0.010
565	17699	2.194	3.224	0.010

(continued)

(Tab. 1 continued)

nm	cm^{-1}	eV	n	k
570	17544	2.175	3.203	0.009
575	17391	2.156	3.187	0.007
580	17241	2.138	3.172	0.005
585	17094	2.119	3.159	0.004
590	16949	2.101	3.148	0.005
595	16807	2.084	3.137	0.008
600	16667	2.066	3.126	0.005
605	16529	2.049	3.117	0.005
610	16393	2.033	3.107	0.005
615	16260	2.016	3.098	0.005
620	16129	2.000	3.090	0.004
625	16000	1.984	3.084	0.003
630	15873	1.968	3.077	0.002
635	15748	1.953	3.071	0.001
640	15625	1.937	3.066	0.002
645	15504	1.922	3.060	0.003
650	15385	1.907	3.054	0.004
655	15267	1.893	3.047	0.005
660	15152	1.879	3.040	0.004
665	15038	1.864	3.033	0.004
670	14925	1.851	3.027	0.004
675	14815	1.837	3.022	0.004
680	14706	1.823	3.016	0.003
685	14599	1.810	3.012	0.003
690	14493	1.797	3.007	0.002
695	14388	1.784	3.004	0.000
700	14286	1.771	3.001	0.000
705	14184	1.759	2.999	0.000
710	14085	1.746	2.996	0.000
715	13986	1.734	2.994	0.001
720	13889	1.722	2.991	0.003
725	13793	1.710	2.986	0.004
730	13699	1.698	2.982	0.007
735	13605	1.687	2.976	0.008
740	13514	1.675	2.971	0.007
745	13423	1.664	2.967	0.007
750	13333	1.653	2.961	0.007
755	13245	1.642	2.959	0.006
760	13158	1.631	2.954	0.006
765	13072	1.621	2.950	0.005
770	12987	1.610	2.947	0.005
775	12903	1.600	2.944	0.003
780	12821	1.590	2.941	0.003
785	12739	1.579	2.939	0.002
790	12658	1.569	2.936	0.001
795	12579	1.560	2.934	0.000
800	12500	1.550	2.934	0.000
805	12422	1.540	2.934	0.000
810	12346	1.531	2.933	0.000
815	12270	1.521	2.933	0.000
820	12195	1.512	2.932	0.000
825	12121	1.503	2.933	0.000
830	12048	1.494	2.933	0.000
835	11976	1.485	2.929	0.000
840	11905	1.476	2.928	0.000
845	11834	1.467	2.925	0.001
850	11765	1.459	2.923	0.005

Tab. 2. The values of the refractive index n and extinction coefficient k of ZnSe layers.

nm	cm^{-1}	eV	n	k
220	45455	5.636	2.777	1.497
222	45045	5.585	2.757	1.501
224	44643	5.535	2.736	1.509
226	44248	5.486	2.716	1.527
228	43860	5.438	2.704	1.549
230	43478	5.391	2.694	1.571
232	43103	5.344	2.688	1.607
234	42735	5.299	2.687	1.640
236	42373	5.254	2.688	1.695
238	42017	5.209	2.705	1.762
240	41667	5.166	2.754	1.852
242	41322	5.123	2.861	1.931
244	40984	5.081	2.991	1.956
246	40650	5.040	3.121	1.932
248	40323	4.999	3.214	1.883
250	40000	4.959	3.274	1.834
252	39683	4.920	3.319	1.813
254	39370	4.881	3.386	1.813
256	39062	4.843	3.509	1.818
258	38760	4.806	3.668	1.759
260	38462	4.769	3.809	1.619
262	38168	4.732	3.880	1.445
264	37879	4.696	3.896	1.281
266	37594	4.661	3.874	1.141
268	37313	4.626	3.836	1.027
270	37037	4.592	3.790	0.931
272	36765	4.558	3.739	0.855
274	36496	4.525	3.691	0.795
276	36232	4.492	3.642	0.743
278	35971	4.460	3.596	0.702
280	35714	4.428	3.553	0.668
282	35461	4.397	3.514	0.641
284	35211	4.366	3.478	0.619
286	34965	4.335	3.446	0.600
288	34722	4.305	3.417	0.583
290	34483	4.275	3.390	0.567
292	34247	4.246	3.366	0.552
294	34014	4.217	3.344	0.540
296	33784	4.189	3.323	0.527
298	33557	4.161	3.305	0.516
300	33333	4.133	3.286	0.506
303	33003	4.092	3.263	0.491
306	32680	4.052	3.239	0.478
309	32362	4.012	3.218	0.465
312	32051	3.974	3.198	0.453
315	31746	3.936	3.180	0.441
318	31447	3.899	3.164	0.431
321	31153	3.862	3.149	0.421
324	30864	3.827	3.134	0.411
327	30581	3.792	3.121	0.402
330	30303	3.757	3.108	0.394
333	30030	3.723	3.096	0.386
336	29762	3.690	3.085	0.378
339	29499	3.657	3.074	0.370
342	29240	3.625	3.064	0.363
345	28986	3.594	3.055	0.356
348	28736	3.563	3.047	0.349
351	28490	3.532	3.039	0.343
354	28249	3.502	3.032	0.336
357	28011	3.473	3.024	0.330
360	27778	3.444	3.017	0.324
365	27397	3.397	3.006	0.314
370	27027	3.351	2.997	0.305
375	26667	3.306	2.989	0.296
380	26316	3.263	2.984	0.289
385	25974	3.220	2.980	0.281
390	25641	3.179	2.980	0.273
395	25316	3.139	2.988	0.259
400	25000	3.100	2.987	0.230
405	24691	3.061	2.969	0.209
410	24390	3.024	2.953	0.198
415	24096	2.988	2.939	0.191
420	23810	2.952	2.930	0.185
425	23529	2.917	2.923	0.177
430	23256	2.883	2.915	0.169
435	22989	2.850	2.908	0.164
440	22727	2.818	2.904	0.160
445	22472	2.786	2.903	0.157
450	22222	2.755	2.907	0.155
455	21978	2.725	2.924	0.155
460	21739	2.695	2.977	0.127
465	21505	2.666	2.953	0.037

(continued)

(Tab. 2 continued)

nm	cm^{-1}	eV	n	k
470	21277	2.638	2.902	0.010
475	21053	2.610	2.869	0.002
480	20833	2.583	2.843	0.002
485	20619	2.556	2.823	0.002
490	20408	2.530	2.806	0.002
495	20202	2.505	2.793	0.002
500	20000	2.480	2.781	0.002
510	19608	2.431	2.753	0.003
520	19231	2.384	2.738	0.002
530	18868	2.339	2.724	0.002
540	18519	2.296	2.709	0.001
550	18182	2.254	2.696	0.000
560	17857	2.214	2.684	0.000
570	17544	2.175	2.674	0.000
580	17241	2.138	2.665	0.001
590	16949	2.101	2.655	0.001
600	16667	2.066	2.648	0.001
610	16393	2.033	2.640	0.001
620	16129	2.000	2.633	0.001
630	15873	1.968	2.627	0.001
640	15625	1.937	2.620	0.001
650	15385	1.907	2.614	0.001
660	15152	1.879	2.609	0.000
670	14925	1.851	2.603	0.000
680	14706	1.823	2.598	0.000
690	14493	1.797	2.594	0.000
700	14286	1.771	2.590	0.000
710	14085	1.746	2.586	0.000
720	13889	1.722	2.583	0.000
730	13699	1.698	2.579	0.000
740	13514	1.675	2.576	0.000
750	13333	1.653	2.573	0.000
760	13158	1.631	2.570	0.000
770	12987	1.610	2.567	0.000
780	12821	1.590	2.564	0.000
790	12658	1.569	2.561	0.000
800	12500	1.550	2.558	0.000
810	12346	1.531	2.555	0.000
820	12195	1.512	2.551	0.000
830	12048	1.494	2.551	0.000
840	11905	1.476	2.548	0.000
850	11765	1.459	2.548	0.000

References

[1] Y. D. Kim, S. L. Cooper, M. V. Klein, B. T. Jonker: *Appl. Phys. Lett.* **62** (1993) 2387

[2] R. Dahmani, L. Salamanca-Riba, N. V. Nguyen, D. Chandler-Horowitz, B. T. Jonker: *J. Appl. Phys.* **76** (1994) 514

[3] C. C. Kim, S. Sivananthan: *Phys. Rev. B* **53** (1996) 1475

[4] M. S. Koo, T. J. Kim, M. S. Lee, M. S. Oh, Y. D. Kim, S. D. Yoo, D. E. Aspnes, B. T. Jonker: *Appl. Phys. Lett.* **77** (2000) 3364

[5] Y. D. Kim, S. G. Choi, M. V. Klein, S. D. Yoo, D. E. Aspnes, S. H. Xin, J. K. Furdyna: *Appl. Phys. Lett.* **70** (1997) 610

[6] D. Franta, I. Ohlídal, P. Klapetek, A. Montaigne-Ramil, A. Bonanni, D. Stifter, H. Sitter: *J. Appl. Phys.* **92** (2002) 1873

[7] D. Franta, I. Ohlídal, P. Klapetek, A. Montaigne-Ramil, A. Bonanni, D. Stifter, H. Sitter: submitted for publication

[8] C. M. Herzinger, B. Johs, W. A. McGahan, J. A. Woollam, W. Paulson: *J. Appl. Phys* **83** (1998) 3323

[9] D. Franta, I. Ohlídal: *Acta Phys. Slov* **50** (2000) 411

[10] D. Franta, L. Zajíčková, I. Ohlídal, J. Janča: *Vacuum* **61** (2001) 279

[11] D. Franta, L. Zajíčková, I. Ohlídal, J. Janča, K. Veltruská: *Diamond Relat. Mater.* **11** (2002) 105

[12] I. Ohlídal, K. Navrátil, F. Lukeš: *J. Opt. Soc. Amer.* **61** (1971) 1630

[13] D. E. Aspnes, G. P. Schwartz, G. J. Gualtieri, A. A. Studna, B. Schwartz, *J. Electrochem. Soc.* **128** (1981) 590

[14] I. Ohlídal, D. Franta: in *Progress in Optics XLI* edited by E. Wolf, North-Holland, Amsterdam (2000), pp 181-282

[15] Ohlídal I., D. Franta: *Acta Phys. Slov.* **50** (2000) 489

[16] S. O. Rice: *Commun. Pure. Appl. Math.* **4** (1951) 351

[17] D. Franta, I. Ohlídal: *J. Mod. Opt.* **45** (1989) 903

[18] D. Franta, I. Ohlídal: in *Proc. 12th Czech-Slovak-Polish Optical Conference on Wave and Quantum Aspects of Contemporary Optics* 2001, SPIE Vol. 4356, p. 207

[19] J. B. Theteen, D. E. Aspnes, R. P. H. Chang: *J. Appl. Phys.* **49** (1978) 6079